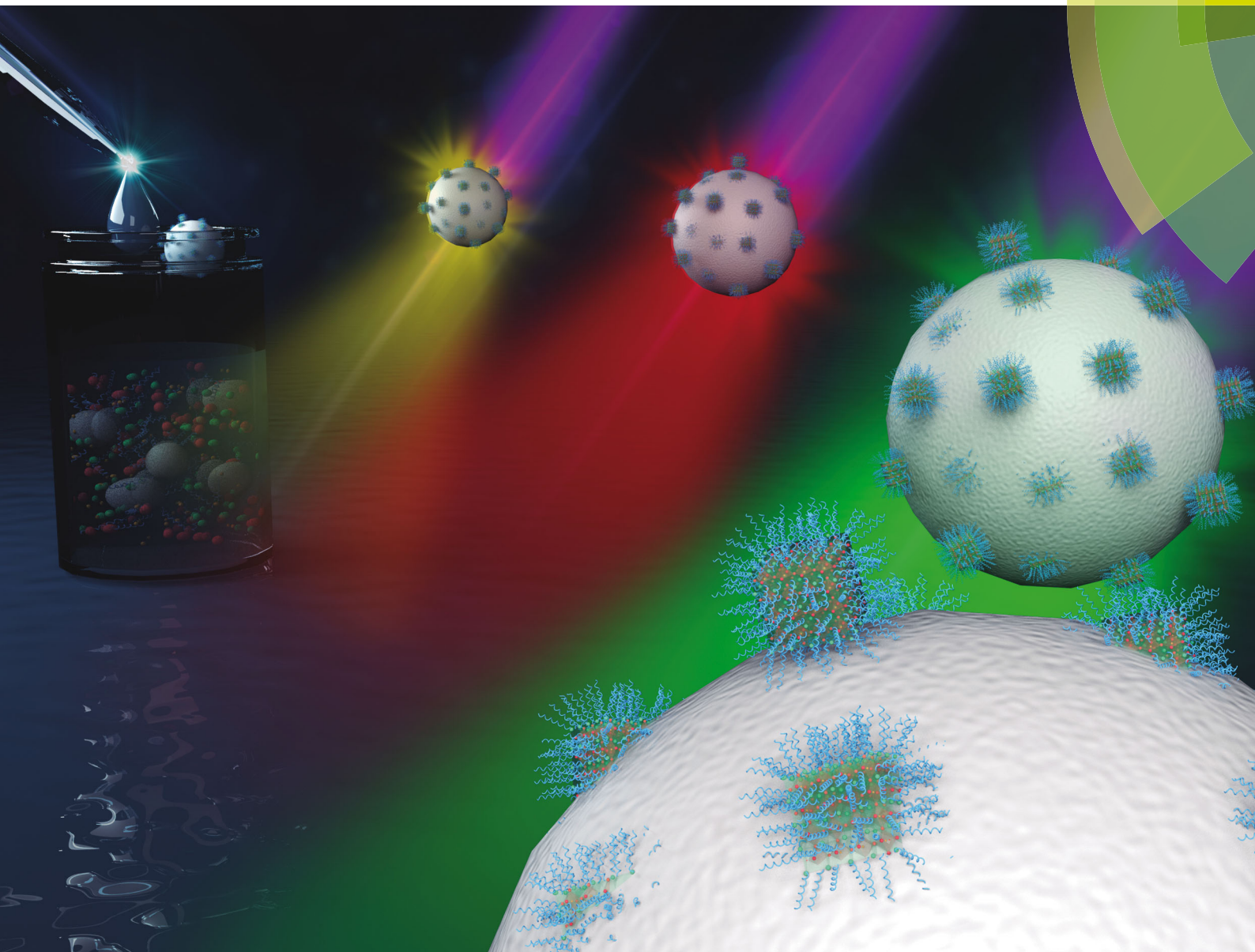


Journal of Materials Chemistry C

Materials for optical, magnetic and electronic devices

rsc.li/materials-c



ISSN 2050-7526



ROYAL SOCIETY
OF CHEMISTRY

Celebrating
IYPT 2019

COMMUNICATION

Yajie Dong *et al.*
Light diffusing, down-converting perovskite-on-polymer
microspheres

Light diffusing, down-converting
perovskite-on-polymer microspheres†Caicai Zhang,[‡] Ziqian He,^{‡c} Hao Chen,^{ac} Le Zhou,^b Guanjun Tan,^c
Shin-Tson Wu^{‡c} and Yajie Dong^{‡*abc}Cite this: *J. Mater. Chem. C*, 2019,
7, 6527Received 27th February 2019,
Accepted 26th March 2019

DOI: 10.1039/c9tc01130g

rsc.li/materials-c

Remote downconverters such as phosphors or quantum dots that are physically separated from blue light-emitting diode (LED) chips can strongly enhance the luminescence efficiency of solid-state lighting (SSL) and liquid-crystal displays (LCDs) because of their reduced light reabsorption. However, the high cost of traditional remote downconverters has limited their wide adoption in these applications. Herein, we report a one-step, general synthesis method that can convert commercial light-diffusing polymer microspheres into highly luminescent perovskite-based downconverters at an extremely low cost. Involving quick anti-solvent-induced heterogeneous nucleation, this method creates well-dispersed perovskite nanoparticles anchored onto polymer microspheres and the whole process takes only several seconds at room temperature without any complex experimental setups. Significantly, the as-synthesized perovskite-on-polymer microspheres (PPMs) offer widely tunable, highly saturated colors with light-diffusing capability. The pure green-emitting CsPbBr₃ manifests a high PL quantum yield of 70.6% and superior stability in water is also demonstrated. Dispersing these PPMs in polydimethylsiloxane (PDMS) resin, we further demonstrate a diffusive downconverting sheet, which is capable of turning blue LEDs into homogeneous light sources with a half-value angle (HVA) as high as 50°. These PPMs hold great promise to be adopted as a low-cost, high-quality replacement for the traditional, expensive remote downconverters in energy efficient SSL, LCDs and beyond.

1. Introduction

In solid-state lighting (SSL) and liquid-crystal display (LCD) backlight systems, homogeneous light sources with desired

primary colors are generally preferred.^{1–3} Traditionally, the light homogeneity and the color conversion are achieved independently. For instance, white-light sources are usually obtained through partial downconversion of blue light-emitting diodes (LEDs) where phosphors^{4,5} or quantum dots (QDs)^{6–8} are applied as the photoluminescent materials. To achieve a homogeneous luminaire, an optical diffuser sheet, with polymer or inorganic light-diffusing microspheres embedded,⁹ is required. Typically, light-diffusing microspheres are made of very low-cost materials. Dispersed into polymer matrices, they can be molded into diffusers with a variety of form factors and these diffusers are often placed remotely from blue LEDs to avoid glare.⁹ Integrating downconverting and light-diffusing capabilities into one component can simplify the optical system design of luminaires and increase their optical efficiency.^{4,5} However, the high cost of traditional phosphors and QD downconverters has prohibited such a remote configuration in SSL since large amounts of expensive materials are needed, which offset the saving gained through efficiency enhancement.¹⁰ Currently, such remote-configured downconverters only find limited applications in high-end LCD backlighting where they are integrated into diffuser films (*e.g.* 3M or Samsung's quantum dot enhanced film, QDEF) to significantly enlarge the display's color gamut.^{6–8} Novel, low-cost, color-tunable downconverters with integrated light diffusion capability are thus highly desirable for highly efficient, high-color-quality SSL and LCD backlights.

Metal halide perovskites (MHPs), particularly those with a chemical formula of APbX₃, where X is generally a halide (F⁻, Cl⁻, Br⁻, I⁻) anion that has stable octahedral coordination with Pb²⁺ to form an extended network of PbX₆ intercalated with larger organic or inorganic cations A such as Cs⁺, CH₃NH₃⁺ (MA⁺) or CH(NH₂)₂⁺ (FA⁺), have recently emerged as important low-cost solar photovoltaic or optoelectronic materials.^{11–13} MHP nanoparticles, synthesized with either hot-injection¹⁴ or ligand-assisted reprecipitation (LARP)^{15,16} have demonstrated high luminescence efficiency, excellent color purity and outstanding color tunability to cover the full range of the visible emission spectrum simply by varying the cation or halide compositions.^{17–25}

^a NanoScience Technology Center, University of Central Florida, Orlando, Florida, 32826, USA. E-mail: Yajie.Dong@ucf.edu

^b Department of Materials Science & Engineering, University of Central Florida, Orlando, Florida 32816, USA

^c College of Optics and Photonics, University of Central Florida, Orlando, Florida 32816, USA

† Electronic supplementary information (ESI) available. See DOI: 10.1039/c9tc01130g

‡ These authors contributed equally.

Despite this progress, instability under external stresses (heat, light and/or water or oxygen in ambient conditions) remains one big challenge to be overcome.^{11,26} For example, MHP nanoparticles often suffer from easy aggregation due to colloidal instability, which will lead to luminescence quenching.^{27–29}

In situ synthesis of MHP nanoparticles in or on a polymer or inorganic matrix can possibly protect them from external stresses and prevent their aggregation, and thus holds great promise for their stabilization.^{24,25,30–32} MHP nanoparticle-polymer composite films fabricated with either a controllable drying process^{33,34} or a swelling-deswelling microencapsulation strategy^{35,36} have recently led to downconverting films with outstanding optical quality and excellent environmental stability. More interestingly, the matrix in microsphere form could bring additional light diffusion functions. Commercial organosilicone microspheres or surface-modified silica nanoparticles were explored as nucleation sites for MHP nanocrystal formation control^{30,31} to form MHP-particle composites in a high temperature synthesis. However, due to their inert surfaces, the composites of MHP and the commercial organosilicone light diffusing agent turned out to manifest much lower PL intensity comparing to those with surface-modified silica nanoparticles,³⁰ and the integration of downconversion with light diffusing capability remains challenging.

Herein, we report a one-step, room-temperature general strategy to convert low cost commercial light-diffusing polymer microspheres into stable MHP-based downconverters with tunable narrow-band emission covering the entire visible spectral range. We show that by an antisolvent-induced heterogeneous nucleation process, ligand-protected MHP nanocrystals can be synthesized, anchored and stabilized on the surface of commercial hydrophobic light-diffusing polymer microspheres. Further experiments and characterization prove that these down-converting perovskite-on-polymer microspheres (PPMs) exhibit excellent color purity, outstanding color tunability, high

water-resistance, long-term stability and integrated light diffusion capabilities.

2. Results and discussion

As schematically shown in Fig. 1a and demonstrated in ESI† V1, commercial light-diffusing polymer microspheres (Sekisui Plastics, Techpolymers) were first dispersed in MHP precursor (CsX and PbX₂, X = Cl⁻, Br⁻, I⁻) solutions with a mixture of oleylamine (OAm) and oleic acid (OA) added as surfactants. Then, an anti-solvent (*e.g.* isopropyl alcohol (IPA)) was quickly injected into the stirred dispersion to induce immediate perovskite nanocrystal nucleation on the polymer microspheres. The formation of PPMs can be accomplished within several seconds at room temperature. After further simple centrifugation and vacuum drying, light-diffusing, downconverting microspheres can be obtained (see the ESI† for experimental details).

The process is generic and can be applied to CsPbX₃ precursor solutions with different halide components X (Cl, Br, I) to achieve widely tunable bandgaps. As depicted in Fig. 1b, a series of CsPbX₃-polymer samples can be synthesized through simple anion tuning, where vivid color can be observed under UV exposure (composition listed in Table S1, ESI†). As expected, the CsPbBr₃ sample exhibits pure green emission. By increasing the stoichiometry ratio of chloride and iodide anions, the emission can be shifted to shorter and longer wavelengths, respectively, and the entire visible range can be covered.

Several key components in this one-step synthesis process are the anti-solvents, surfactants OAm and OA and commercial light-diffusing polymer microspheres. They work synergistically and play important roles in determining the nucleation, growth, dispersion and stabilization of MHP nanoparticles on the diffusing, downconverting PPMs.

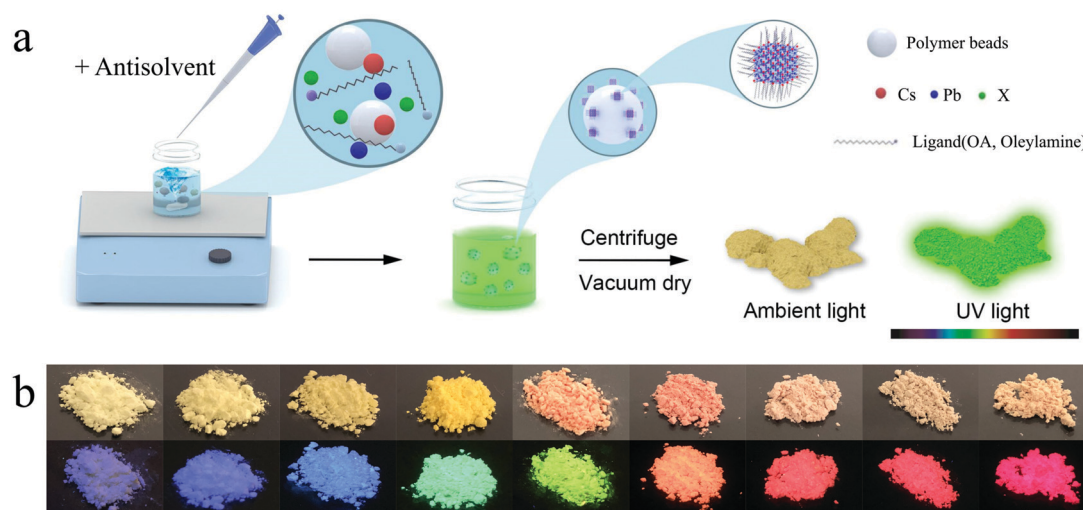


Fig. 1 Schematic illustration of the fabrication process of light-diffusing, downconverting perovskite-on-polymer microspheres (PPMs). (a) After a one-step synthesis of PPMs through antisolvent-induced heterogeneous nucleation, the powders can be obtained by further centrifugation and vacuum drying. (b) Images of PPMs with different anion compositions under ambient light (upper) and 365 nm UV light (lower) illumination.

Anti-solvents can drastically reduce the solubility of MHP in the precursor solution, driving the perovskite precursor into supersaturation or metastable zones to induce crystal nucleation.³⁷ Previously, anti-solvents have been employed for the growth of high-quality MHP single crystals³⁸ or polycrystalline thin films³⁹ in MHP photovoltaic research. The anti-solvent compositions and/or amounts often need to be carefully optimized for controlled crystalline growth.⁴⁰ For luminescent MHP nanocrystal growth, additional surfactant ligands (OAm and OA) are often necessary to provide further kinetic control of the nucleation and growth processes, as in the LARP synthesis of freestanding MHP nanocrystals.¹⁵ Even with the ligands, the LARP synthesis yield remains low and as-synthesized MHP nanocrystals tend to aggregate easily upon aging or processing.⁴¹

In our instance, commercial light-diffusing polymer microspheres provide the third important control parameter for the otherwise drastic anti-solvent induced crystallization process. In the synthesis, the surfaces of these microspheres will act as heterogeneous nucleation sites to effectively lower the nucleation energy of MHP nanoparticles.^{42,43} Also, ligand protected MHP nuclei can be anchored onto the surface of the hydrophobic microspheres, preventing MHP nanoparticles from further aggregation and luminescence quenching in the subsequent growth, as continuing growth of MHP nanoparticles will lead to more defects in the crystal structure.⁴¹ Such well dispersed MHP nanoparticles possess high luminescence with an outstanding color coverage range. As a control, when the synthesis was carried out under otherwise identical conditions, but without the polymer microsphere matrix, the luminescence of the as-obtained products is generally much lower and MHP nanoparticles supposedly emitting some colors, such as red, cannot even be formed because of particle aggregation (Fig. S1, ESI†).

In addition, these commercial light-diffusing polymer microspheres have been widely used in SSL and LCD industries⁴⁴ and are expected to provide high light diffusivity, low light transmission loss and uniform lighting brightness. The composition of the polymer powders can include highly crosslinked polystyrene (PS) or polymethylmethacrylate (PMMA) that has low solubility in the solvent, which in most cases is *N,N*-dimethylformamide (DMF). The size of the polymer microspheres can also vary, ranging from 1 to 8 μm in our experiment, indicating widely tunable light diffusion capabilities. With all these very low-cost components and the simple process fulfilled at room temperature, this synthesis method proves to be very economical and scalable.

Optical characterization reveals the outstanding color purity and tunability of these PPMs. Photoluminescent (PL) spectra of the samples and their corresponding CIE 1931 color coordinates are also plotted in Fig. 2a and b, respectively, and the peak energy change with the halide anion fraction can be found in Fig. S2 (ESI†). The emission colors can be tuned from deep blue (453 nm) to deep red (662 nm) with a full width at half maximum (FWHM) ranging from 12.5 nm to 37 nm, which ensures highly saturated colors covering the entire Rec. 2020 color space (Table S1, ESI†). Among them, the pure green-emitting CsPbBr_3 manifests a high PL quantum yield of 70.6%, and pure red-emitting $\text{CsPbBr}_{0.42}\text{I}_{2.58}$ -PS particles ($x = 0.75$) manifest a PL quantum yield of 40.5%.

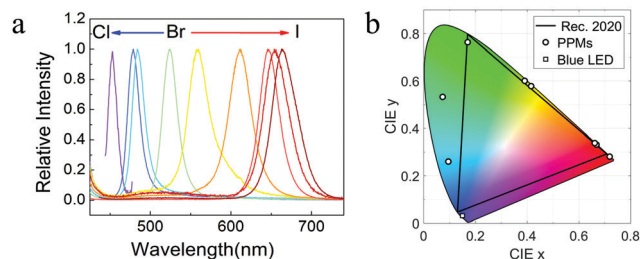


Fig. 2 Optical properties of downconverting perovskite-on-polymer microspheres (PPMs) (a) photoluminescence spectra of the samples under UV excitation; (b) corresponding CIE1931 color coordinates of the samples under blue LED excitation.

To reveal the crystal structure of the perovskite-on-polymer microspheres, X-ray diffraction (XRD) characterization was carried out. As shown in Fig. 3, even in the presence of broad background noise from the polymer microsphere matrix, signals from the crystalline CsPbX_3 can be clearly distinguished. With the anion modification, the CsPbX_3 crystal structure will transition from three-dimensional (3D) perovskite structures with connected PbX_4 octahedra ($\text{CsPbCl}_x\text{Br}_{3-x}$ and CsPbBr_3) to a one-dimensional (1D) wider-gap (yellow) phase with an orthorhombic lattice type ($\text{CsPbBr}_x\text{I}_{3-x}$), which is consistent with previous reports.⁴⁵ The dotted line in Fig. 3 highlights the gradual shift of peak (110) of the 3D perovskite phase. As expected, compared to CsPbBr_3 -based PPMs, the samples with a larger ratio of chloride ions have a relatively small unit structure, resulting in a larger diffraction angle. On the other hand, samples with an increased ratio of iodine ions have a larger unit structure, which leads to a smaller diffraction angle. With a significantly increased iodine component (e.g. $\text{CsPbBr}_{0.42}\text{I}_{2.58}$), the 1D yellow phase becomes dominant. However, the PPMs remain luminescent, indicating nanocrystals of the 3D perovskite phase probably still form, although at a ratio

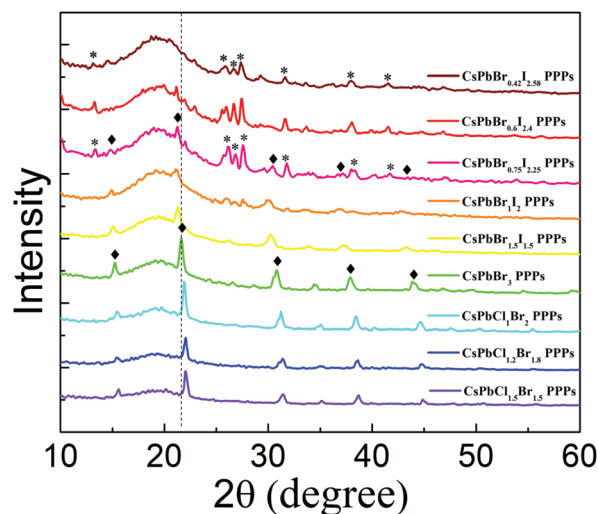


Fig. 3 XRD patterns of PPM samples obtained with 8 μm crosslinked PS powders. The dotted line highlights the shift of the (110) peak of the 3D perovskite crystal structure with the anion composition changes. ♦ indicates peaks of the 3D perovskite structure; * indicates peaks of the 1D orthorhombic phase structure.

too low to be effectively detected with XRD. Further investigation illustrates that all the CsPbBr₃ nanocrystal formations are compatible with different kinds of polymer microspheres such as PS and PMMA whose size ranges from 1 to 8 μm (Fig. S3, ESI†), indicating the common roles of different polymer microspheres in the synthesis.

In addition to XRD, more details of PPMs can be discovered through other microscopic characterization. As shown in Fig. 4a and b, the fluorescent optical microscope images indicate that the red and green photoluminescent perovskite nanocrystals were spread around the 8 μm PS particles mostly homogeneously. For the red samples, besides the luminescent microspheres, rod shaped non-luminescent microcrystals are visible in bright-field imaging (Fig. S4, ESI†), which have contributed to the major 1D yellow phase with an orthorhombic lattice. Meanwhile, the scanning electron microscopy (SEM) images in Fig. 4c and Fig. S5 (ESI†) disclose that the perovskite nanoparticles are indeed anchored on the surface of the PS polymer microspheres and separated from each other. The transmission electron microscopy (TEM) characterization in Fig. 4d also confirmed the anchoring effect, and the energy-dispersive X-ray spectroscopy (EDS) characterization on the surface anchored nanocrystals has a Cs/Pb/Br molar ratio of 1:1:3.2 (Fig. S6, ESI†), in accordance with the stoichiometry of CsPbBr₃. By further focusing on individual particles, the high-resolution TEM (HRTEM) and fast Fourier transform (FFT) images demonstrate interplanar distances of ~2.64 and ~2.97 Å, which are close to the (210) plane *d*-spacing (2.62 Å) and the (002) plane *d*-spacing (2.94 Å) of 3D CsPbBr₃ perovskites.

Although the abovementioned characterization revealed that most perovskite nanoparticles are only anchored on the polymer microsphere surface and can still be exposed to the external environment, these PPMs are surprisingly stable in water. To test the stability, CsPbBr₃ PPMs were immersed in water and their PL intensity was recorded every 24 hours. As shown in Fig. 5a and Fig. S7 (ESI†), the luminescence decay mainly happened in the first 2–3 days. After immersion in water

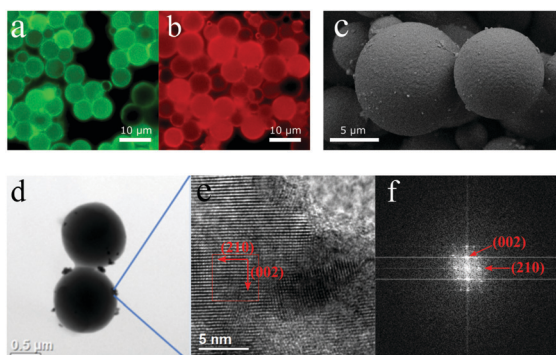


Fig. 4 Microscopic characterization of PPMs. (a) Fluorescent optical microscope image of CsPbBr₃-PS particles with an average size of 8 μm under UV excitation. (b) Fluorescent optical microscope image of CsPbBr_{3-x}-PS particles (*x* = 0.75) with an average size of 8 μm under UV excitation. (c) SEM image of an 8 μm CsPbBr₃-PS particle. (d) TEM image of CsPbBr₃ NCs anchored onto the surface of a 1 μm PMMA particle with (e) the corresponding HRTEM image and (f) FFT image.

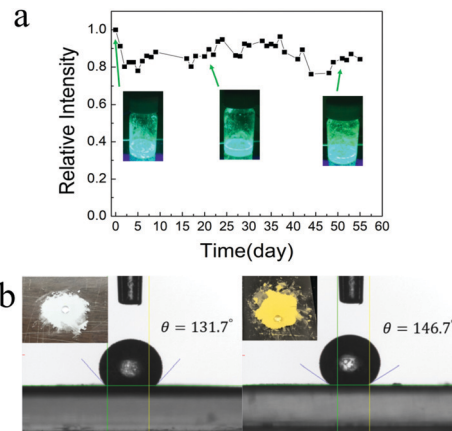


Fig. 5 The water resistance test of PPMs. (a) PL intensity variations of the CsPbBr₃-PS powders immersed in water for over 50 days, instrumental errors could contribute to the PL intensity fluctuation. (b) Water contact angle measurements for plain 8 μm PS powder and CsPbBr₃-PS 8 μm powder.

for over 50 days, the green samples maintained 75–80% of their original PL intensity (Fig. 5a), and the emission peak remained unchanged (Fig. S8, ESI†). Even for the red samples, which normally show much worse stability,⁴⁶ the PL intensity still maintained ~60% of the initial value (Fig. S7, ESI†), and the emission peak stayed the same (Fig. S9, ESI†). The decay in the first 2–3 days is mainly related to the luminescence quenching of the freestanding MHP nanocrystals. In our fabrication process, with polymer microsphere surfaces as MHP nucleation sites, the majority of the perovskite nanocrystals will be formed and attached at the microsphere surfaces. But there will be some of them formed as “free” perovskite nanocrystals without any protection of the polymer matrix, which should be less stable, especially for red PPMs as shown in Fig. S4 (ESI†). In addition, the nanocrystals that are attached at the microsphere surfaces are only partially protected by the polymer matrix. The external part of these nanocrystals is more prone to be damaged when they are immersed in water. Meanwhile, iodine-based red MHPs will suffer more from structural instability issues, which is known as the “perovskite red wall” problem, as it is difficult to obtain stable nanocrystals with photoluminescence in the red and near-infrared spectral regions.⁴⁶ On the other hand, we believe the outstanding water stability should be ascribed to (1) the partial protection from highly crosslinked polymers, which slightly swell in perovskite precursor solutions, and (2) the formation of air nanobubbles at the interface between water and the hydrophobic polymer microsphere surface to isolate the perovskite nanocrystals from the water environment. The interaction mechanism should be mainly ascribed to the slight swelling of the highly crosslinked polymers. However, because of their high crosslinking level and solvent resistance, it is anticipated that swelling wouldn't be complete and the majority of anti-solvent induced MHP crystallization will happen at the interface between the polymer microspheres and the solution with MHP nanoparticles only partially protected by the polymer matrix. Fortunately, the hydrophobic nature of the

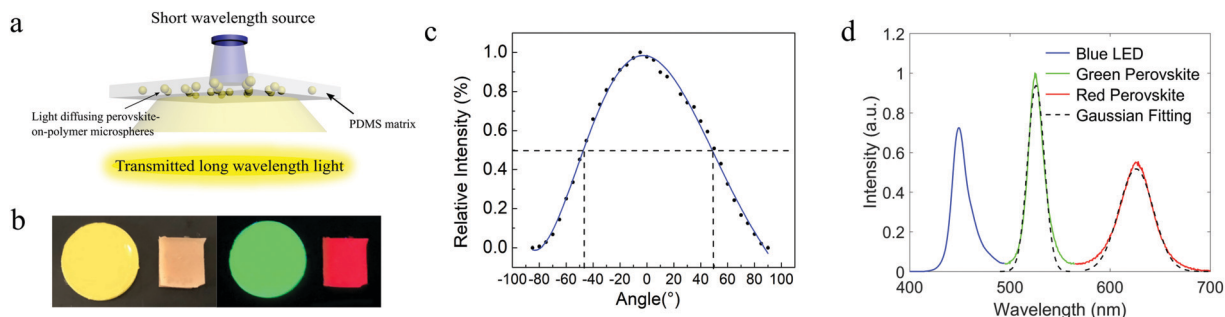


Fig. 6 Application of PPMs as both narrow-band downconverters and light diffusers for lighting systems. (a) Scheme of diffusive white light generation by combining a PPM-in-PDMS film with blue LEDs. (b) Photographs of single-color PPM-in-PDMS films under ambient light (left) and UV light (right) illumination. (c) Half-value-angle measurement results of the PPM-in-PDMS sheets. (d) Emission spectra of a white LED system with green and red PPMs as downconverters pumped by blue LEDs. Dashed lines refer to Gaussian fits of the PPM emission spectra.

polymer microsphere surfaces provides additional protection against water and helps maintain high stability even if the swelling–deswelling microencapsulation is not complete. Based on a previous report,⁴⁷ stable nanobubbles tend to be formed on a solid surface when immersing the substrate into a liquid. Another study illustrated that nanobubbles formed on a hydrophobic surface will be more stable than those formed on a hydrophilic surface.^{48–50}

More interestingly, the perovskite nanocrystal formation on the microsphere surface increases the hydrophobicity of the microsphere itself. Before any treatment, the contact angle between the polymer microsphere and water is 131.7°, indicating good hydrophobicity (Fig. 5b). After the one-step process of the luminescent PPM synthesis, the microsphere shows even better hydrophobicity with the contact angle increased to 146.7° (Fig. 5b), approaching the super hydrophobicity range. This contact angle increment is probably due to the high hydrophobicity of the surfactant OAM attached on the microsphere surface during the nanocrystal formation. With such a high hydrophobicity, the PPM water stability can be further ensured, and even helped the microsphere to survive in boiling water (ESI† V2). In contrast, the green emitting perovskite nanoparticles synthesized without hydrophobic polymer microspheres and with otherwise identical conditions are not stable in water at room temperature (Fig. S10, ESI†).

With the advantages of their process simplicity, extremely low cost, high stability, high luminescence efficiency and excellent color saturation, these PPMs hold great potential for many applications. To demonstrate an example of applying PPMs as both downconverters and diffusers, we buried green CsPbBr₃ and red CsPbBr_xI_{3–x} ($x = 0.75$) luminescent microspheres into polydimethylsiloxane (PDMS) resin, as schematically depicted in Fig. 6a, to make a diffusive down-converting sheet. Fig. 6b shows typical PPM-in-PDMS sheets with a mass ratio of 0.05 mg mg^{–1} and a sheet thickness of around 2 mm. Uniform illumination can be achieved when placing this sheet over a high intensity blue or UV light source.

To further quantify the light diffusion performance of the PPM-in-PDMS sheet, a half-value angle (HVA) test was

implemented. The test is based on measurements of the light intensities at different angles, ranging from –90° to +90° in our experiment.⁵¹ The final half-value angle is determined by the half value of the emitted light intensity with reference to its peak value, which is usually obtained at the normal angle. As observed in Fig. 6c, a half-value angle of 50° can be reached. Such a wide-HVA film is comparable to a highly diffusive sheet for white LEDs.⁵¹ With further optimization of the PPM concentration and the sheet thickness, the performance of the diffusivity and the downconversion can be customized to meet specific requirements for different SSL or LCD backlights. As a prominent example, when the PPM-in-PDMS sheet is pumped by a 450 nm blue LED, the resultant green (524 nm with a FWHM of 22 nm) and red (624 nm with a FWHM of 29 nm) spectra can be well fitted by Gaussian functions, and can match that of the CIE standard illuminant D65 (6504-K correlated color temperature), as shown in Fig. 6d. This white light with narrow-band primary colors makes it ideal for LCD backlights, and thus we believe our downconverting, light-diffusing sheet is promising for displays and holds great potential for other lighting applications where tunable, pure emission is desired.

3. Conclusions

In conclusion, color-tunable PPMs are achieved through a simple antisolvent-induced heterogeneous nucleation process on commercial light-diffusing polymer microspheres. These PPMs demonstrate high stability, high efficiency, excellent color purity, and extremely low cost. Thanks to the light-diffusing property of the microspheres and the color tunability of the MHP, homogeneous and tunable light sources can be realized with as-synthesized PPMs, which ensures the great potential of PPMs in simplifying the optical design for uniform illuminators in emerging SSL or LCD backlights at a very low cost. With further improvements in stability and/or polymer microsphere engineering they can also find other applications such as acting as security phosphors²⁴ or biological imaging agents.⁵²

Conflicts of interest

There are no conflicts to declare.

Acknowledgements

C. Zhang and Z. He contributed equally to this work. The authors thank Dr Yongho Sohn, Dr Lei Zhai, Dr Chen Shen and Materials Characterization Facility AMPAC of University of Central Florida (UCF) for assistance in TEM or SEM characterization and thank Dr Shun-Wei Liu of Mingchi University of Technology for PLQY measurements. We thank Sekisui Plastics for providing techpolymer light diffusing microsphere samples. Y. Dong is grateful for support of this work by UCF through startup funding (Grant No. 20080738) and a NSTC seed grant (No. 63014223).

Notes and references

- J. Brodrick, M. Pattison, N. Bardsley, M. Hansen, L. Pattison, S. Schober, K. Stober, J. Tsao and M. Yamada, DOE Solid-State Lighting 2017 Suggested Research Topics.
- A. Bergh, G. Craford, A. Duggal and R. Haitz, *Phys. Today*, 2001, **54**, 42–47.
- C. F. Chen, LEDs for liquid crystal display (LCD) back-lighting, in *Nitride Semiconductor Light-Emitting Diodes (LEDs)*, ed. J. Huang, H. Kuo and S. Shen, Woodhead Publishing, Duxford, UK, 2nd edn, 2018, p. 619.
- J. K. Kim, H. Luo, E. F. Schubert, J. Cho, C. Sone and Y. Park, *Jpn. J. Appl. Phys., Part 2*, 2005, **44**, 649–651.
- G. Singh and D. S. Mehta, *J. Inf. Disp.*, 2014, **15**, 91–98.
- J. V. Derlofske, J. Schumacher, J. Hillis, D. Lamb, F. McCormick and A. Lathrop, Quantum Dot Enhancement Film (QDEF), 3M White Paper, 2013.
- Z. Luo, Y. Chen and S.-T. Wu, *Opt. Express*, 2013, **21**, 26269–26284.
- R. Zhu, Z. Luo, H. Chen, Y. Dong and S.-T. Wu, *Opt. Express*, 2015, **23**, 23680–23693.
- X. Ouyang, P. Li, D. Chen and J. Tang, *J. Appl. Polym. Sci.*, 2016, **133**, 42923.
- M. C. Leung, White LED and Remote Phosphor Comparison, Cree White Paper, 2014.
- A. Kojima, K. Teshima, Y. Shirai and T. Miyasaka, *J. Am. Chem. Soc.*, 2009, **131**, 6050–6051.
- H. J. Snaith, *J. Phys. Chem. Lett.*, 2013, **4**, 3623–3630.
- S. D. Stranks and H. J. Snaith, *Nat. Nanotechnol.*, 2015, **10**, 391–402.
- L. Protesescu, S. Yakunin, M. I. Bodnarchuk, F. Krieg, R. Caputo, C. H. Hendon, R. X. Yang, A. Walsh and M. V. Kovalenko, *Nano Lett.*, 2015, **15**, 3692–3696.
- F. Zhang, H. Zhong, C. Chen, X. G. Wu, X. Hu, H. Huang, J. Han, B. Zou and Y. Dong, *ACS Nano*, 2015, **9**, 4533–4542.
- X. Li, Y. Wu, S. Zhang, B. Cai, Y. Gu, J. Song and H. Zeng, *Adv. Funct. Mater.*, 2016, **26**, 2435–2445.
- S. Pathak, N. Sakai, F. W. R. Rivarola, S. D. Stranks, J. Liu, G. E. Eperon, C. Ducati, K. Wojciechowski, J. T. Griffiths, A. A. Haghighirad, A. Pellaroque, R. H. Friend and H. J. Snaith, *Chem. Mater.*, 2015, **27**, 8066–8075.
- Y. Bekenstein, B. A. Koscher, S. W. Eaton, P. Yang and A. P. Alivisatos, *J. Am. Chem. Soc.*, 2015, **137**, 16008–16011.
- H. Huang, A. S. Susha, S. V. Kershaw, T. F. Hung and A. L. Rogach, *Adv. Sci.*, 2015, **2**, 1500194.
- M. C. Weidman, M. Seitz, S. D. Stranks and W. A. Tisdale, *ACS Nano*, 2016, **10**, 7830–7839.
- B. R. Sutherland and E. H. Sargent, *Nat. Photonics*, 2016, **10**, 295–302.
- I. Levchuk, A. Osvet, X. Tang, M. Brandl, J. D. Perea, F. Hoegl, G. J. Matt, R. Hock, M. Batentschuk and C. J. Brabec, *Nano Lett.*, 2017, **17**, 2765–2770.
- G. Gao, Q. Xi, H. Zhou, Y. Zhao, C. Wu, L. Wang, P. Guo and J. Xu, *Nanoscale*, 2017, **9**, 12032–12038.
- L. Xu, J. Chen, J. Song, J. Li, J. Xue, Y. Dong, B. Cai, Q. Shan, B. Han and H. Zeng, *ACS Appl. Mater. Interfaces*, 2017, **9**, 26556–26564.
- Y. Wei, X. Deng, Z. Xie, X. Cai, S. Liang, P. Ma, Z. Hou, Z. Cheng and J. Lin, *Adv. Funct. Mater.*, 2017, **27**, 1703535.
- H. Cho, Y.-H. Kim, C. Wolf, H.-D. Lee and T.-W. Lee, *Adv. Mater.*, 2018, **30**, 1704587.
- T. Leijtens, G. E. Eperon, N. K. Noel, S. N. Habisreutinger, A. Petrozza and H. J. Snaith, *Adv. Energy Mater.*, 2015, **5**, 1500963.
- G. Niu, X. Guo and L. Wang, *J. Mater. Chem. A*, 2015, **3**, 8970–8980.
- T. A. Berhe, W. N. Su, C. H. Chen, C. J. Pan, J. H. Cheng, H. M. Chen, M. C. Tsai, L. Y. Chen, A. A. Dubale and B. J. Hwang, *Energy Environ. Sci.*, 2016, **9**, 323–356.
- X. Li, Y. Wang, H. Sun and H. Zeng, *Adv. Mater.*, 2017, **29**, 1701185.
- X. Li, K. Zhang, J. Li, J. Chen, Y. Wu, K. Liu, J. Song and H. Zeng, *Adv. Mater. Interfaces*, 2018, **5**, 1800010.
- C. Zhang, J. He, H. Chen, G. Tan, L. Zhou, S. Wu, Y. Sohn and Y. Dong, *SID Int. Symp. Dig. Tech. Pap.*, 2018, **49**, 222–224.
- S. Chang, Z. Bai and H. Zhong, *Adv. Opt. Mater.*, 2018, **6**, 1800380.
- Q. Zhou, Z. Bai, W. G. Lu, Y. Wang, B. Zou and H. Zhong, *Adv. Mater.*, 2016, **28**, 9163–9168.
- Y. Wang, J. He, H. Chen, J. Chen, R. Zhu, P. Ma, A. Towers, Y. Lin, A. J. Gesquiere, S. T. Wu and Y. Dong, *Adv. Mater.*, 2016, **28**, 10710–10717.
- J. He, A. Towers, Y. Wang, P. Yuan, J. Zhang, J. Chen, A. J. Gesquiere, S.-T. Wu and Y. Dong, *Nanoscale*, 2018, **10**, 15436–15441.
- M. Konstantakou, D. Perganti, P. Falaras and T. Stergiopoulos, *Crystals*, 2017, **7**, 291.
- Y. Tidhar, E. Edri, H. Weissman, D. Zohar, G. Hodes, D. Cahen, B. Rybtchinski and S. Kirmayer, *J. Am. Chem. Soc.*, 2014, **136**, 13249–13256.
- N. J. Jeon, J. H. Noh, Y. C. Kim, W. S. Yang, S. Ryu and S. I. Seok, *Nat. Mater.*, 2014, **13**, 897–903.
- K. M. Lee, C. J. Lin, B. Y. Liou, S. M. Yu, C. C. Hsu, V. Suryanarayanan and M. C. Wu, *Sol. Energy Mater. Sol. Cells*, 2017, **172**, 368–375.

- 41 F. Zhu, L. Men, Y. Guo, Q. Zhu, U. Bhattacharjee, P. M. Goodwin, J. W. Petrich, E. A. Smith and J. Vela, *ACS Nano*, 2015, **9**, 2948–2959.
- 42 C. Li, Z. Zang, C. Han, Z. Hu, X. Tang, J. Du, Y. Leng and K. Sun, *Nano Energy*, 2017, **40**, 195–202.
- 43 T. Geske, J. Li, M. Worden, X. Shan, M. Chen, S. G. R. Bade and Z. Yu, *Adv. Funct. Mater.*, 2017, **27**, 1702180.
- 44 <http://www.tech-p.com/en/about/index.html>, accessed: December, 2018.
- 45 C. H. Lu, J. Hu, W. Y. Shih and W. H. Shih, *J. Colloid Interface Sci.*, 2016, **484**, 17–23.
- 46 L. Protesescu, S. Yakunin, S. Kumar, J. Bär, F. Bertolotti, N. Masciocchi, A. Guagliardi, M. Grotevent, I. Shorubalko, M. I. Bodnarchuk, C. J. Shih and M. V. Kovalenko, *ACS Nano*, 2017, **11**, 3119–3134.
- 47 Y. Sun, G. Xie, Y. Peng, W. Xia and J. Sha, *Colloids Surf., A*, 2016, **495**, 176–186.
- 48 X. H. Zhang, N. Maeda and V. S. J. Craig, *Langmuir*, 2006, **22**, 5025–5035.
- 49 X. H. Zhang, A. Quinn and W. A. Ducker, *Langmuir*, 2008, **24**, 4756–4764.
- 50 G. Pan and B. Yang, *ChemPhysChem*, 2012, **13**, 2205–2212.
- 51 G. Bar and M. Nir, *Plastic Light diffusion systems match LED lighting needs*, *LEDs Magazine*, 2017, July/August, pp. 33–37.
- 52 M. P. Robin and R. K. O'Reilly, *Polym. Int.*, 2015, **64**, 174–182.